Chalcogenide Letters Vol. 21, No. 11, November 2024, p. 873 - 884

A simplified study on physical and mechano-structural properties of newly produced Sm^{3+} doped zinc telluro-phosho-borate glasses

Areej S. Alqarni [a,*], I. Bulus[b], M. Abioye[c]
[a]*Department of Physics, College of Science, Princess Nourah Bint Abdulrahman University, P.O. Box 84428, Riyadh 11671, Saudi Arabia*
[b]*Department of Physics, Kaduna State College of Education Gidan waya, Kafanchan, Nigeria*
[c]*Department of Mechanical Engineering, Kogi State Polytechnic, Lokoja, Nigeria*

To unveiled the function of exchanging Sm_2O_3 for B_2O_3 on the physical and mechano-structural traits of multi-component glass, five distinct type (A, B, C, D and E) of glasses originated from (50-x)B_2O_3-10P_2O_5-30TeO_2-10ZnO-$x$$Sm_2O_3$ ($0.1 \leq x \leq 1.5$, mol%) compositions were fabricated by using ordinary approach of melt-quenching. The non-crystallinity status of the synthesized samples was established by X-ray diffraction (XRD) profile. However, with sequential replacement of B_2O_3 by Sm_2O_3, the deduced values of physical entities such as density (d_s), Sm^{3+} ions concentration (N_i), field strength (F) and glass hardness (H_V) of our produced glasses were significantly amplified, while the molar volume (V_m) alongside polaron radius (r_p) and inter-nuclear distance (r_i) decline. Besides, data from FTIR with consequential deconvoluted spectral showcased the presence of BO_3, BO_4, TeO_3, TeO_4 and PO_4 functional groups which were randomly distributed within the main glass network.

(Received July 15, 2024; Accepted November 6, 2024)

Keywords: New type of glasses, Samarium oxide, Vickers hardness, Structural properties

1. Introduction

The present and futuristic applications of glassy materials have impelled a gigantic research interest on the fabrication of novel glasses with an exclusive physical, mechanical and structural qualities [1], [2], [3], [4]. Obtainable literature declared that the feature of glass system such as physical, mechanical, structural and optical are strongly controlled by its composition wherein multi-component glass host containing two or more network formers presented better and stable structured [5], [6], [7]. In view of this assertion, curiosity has been generated lately on physical and structural investigations of complex glasses amalgamated with borate, tellurite and phosphate concurrently [8], [9]. In 2010, Mosner and his companion [10] studied the structure of ZnO–B_2O_3–P_2O_5–TeO_2 glasses. The said glasses unequivocally present enhanced properties like favourable melting points, elevated densities, unique chemical durability and stability [10]. These assets indeed offer huge potentials and are ever-demanding in numerous areas like high strength glass for internal electronics protector, memory devices and optical fiber amplifiers [11]. Unluckily, studies on the structural attributes of ZnO– B_2O_3–P_2O_5–TeO_2 glasses to the best of authors knowledge is absolutely undersupplied. Although, Selvi and his team mates in 2014 [12], 2015 [13] and 2016 [14], respectively, scientifically examined the structure-optical characteristics of boro-telluro-phosphate glass system. Since then, researched on the aforementioned glass host remains stagnant until 2021 where Qian et al [15] inspected PbO effect as modifier on the traits of gamma ray shielding for boro-telluro-phosphate glasses. Afterwards, the role of modifiers on spectral qualities of boro-telluro-phosphate glasses implanted with dysprosium ions for W-LEDs utilization was scrutinized and broadcasted by Poojha and his fellows [16]. Bearing in mind that the augmentations of the glass potentials involves profound understanding of the glass structure as deliberated in the above-mentioned studies, a gap on structural, mechanical and physical information need to be filled.

* Corresponding author: arsalqarni@pnu.edu.sa
https://doi.org/10.15251/CL.2024.2111.873

Furthermore, it has been well established that insertion of samarium ions in the glass matrix supplements the structural and luminescence behaviour and henceforth, opening opportunities in finding fresh applications [17], [18], [19]. This pronouncement undeniably makes physical and structural investigations of glasses containing Sm_2O_3 indispensable.

In this view, we considered a novel composition of ZnO– B_2O_3–P_2O_5–TeO_2 glass to be interesting matrix for samarium oxide doping. Therefore, the present study aims to investigate the physical and mechano-structural properties of fresh zinc telluro-phospho-borate glasses implanted with varying content of Sm_2O_3. To this end:

i. Five 5 samples of Sm_2O_3 infused zinc telluro-phospho-borate glasses have been synthesized.

ii. The densities of the fabricated glass samples were measured and molar volume (V_M) haven been deduced.

iii. The glassy phase of the as-prepared samples was inspected via X-ray diffraction (XRD) measurements.

iv. The structural modifications induced by Sm_2O_3 and its influence on the hardness traits of the present glasses was scrutinized by FTIR and vicker hardness analyses.

2. Experimental materials and methods

2.1. Glass samples fabrication

In this work, the multi-component glass compositions typified by the following standard formulation: (50-x)B_2O_3-10P_2O_5-30TeO_2-10ZnO- $x$$Sm_2O_3$ with x taking the values of 0.1, 0.5, 0.7, 1.0 and 1.5 mol% embodied as glass A, glass B, glass C, glass D and glass E, respectively, were fabricated via classic melt-quenching approach using high purity (≥99.99%) ZnO, B_2O_3, P_2O_5, TeO_2 and Sm_2O_3 as preparatory materials. The maiden materials, weighed based on designed proportions were ground and thoroughly mixed. The resultant mixture (batches) about in an alumina crucible were melted at 1150 °C for 90 minutes. Thereafter, the uniformly melt was poured into a preheated copper in the low temperature furnace and annealed at 350 °C for 3 h.

2.2. Instrumentations

To ascertain the physical attributes of the current glass system, the density of glass samples was quantified through the principle of Archimedes wherein toluene was utilized as immersion liquid. Besides, the inspection of non-crystalline state of the newly produced samples was conducted by using X-ray diffractometer (model, Philips X'Pert) with a Cu Ka radiation of wavelength k = 1.54056 Å for 2h angles between 10 and 80°. Conversely, micro-indentation analysis was performed on the entire glasses with 50, 100,200, 300 and 500 g applied loads via digital microhardness tester (Shimadzu HVM-2). Above and beyond, the existence of different functional groups was verified with the aid of FTIR spectrophotometer (Perkin Elmer, model) in the 400–4000 cm^{-1} wavenumber range.

2.3. Theoretical formulations for deducing physical and structural parameters

2.3.1. Evaluation of density and molar volume

As discussed in the outgoing section, the density of our newly glass samples (d_s) are deduced as follows [20].

$$d_s = \left[\frac{W_{SA}}{W_{SA}-W_{SL}}\right] \times d_L \tag{1}$$

where the abbreviations d_s and $d_L$stand for density of the sample and liquid, while W_{SA} and W_{SL} are corresponding weight of glass in air and in liquid. However, by utilizing the attained d_s, molar volume (V_m) of the glass samples can be deduced as follows [21]:

$$V_m = \sum \frac{n_{iM_i}}{d_s} \tag{2}$$

Here, M_i = molecular weight for a component I and n_i = molar fraction.

Basing on the acquired values of d_s and V_m, other crucial physical quantities are computed using the following expressions:

The Sm^{3+}ions concentration, N_i is given as [22]:

$$N_i = \frac{n_i\, d_s N}{M_a} \tag{3}$$

where N = Avogadro's number, n_i = mole fraction and $M_a$is the average molecular weight of the prepared sample Polaron radius [22]:

$$r_p(\text{Å}) = \frac{1}{2}\left(\frac{\pi}{6N_i}\right)^{1/3} \tag{4}$$

Inter-nuclear distance [23]:

$$r_i(\text{Å}) = \left(\frac{1}{N_i}\right)^{1/3} \tag{5}$$

Field strength (F) [24]:

$$\text{F} = \frac{Z}{r_p^2} \tag{6}$$

Here, Z denotes atomic number of samarium ion.

2.3.2. Computation of mechanical parameters

In this work, the values of micro-hardness were computed Vickers geometry formula below [25]:

$$H_V = \frac{1.8544P}{d^2} \tag{7}$$

Here, the symbol H_V designate micro-hardness number measured kg/mm^2, the normal load deduced in kg is represented by P, and d denotes mean diagonal length of the indentation in mm.

2.3.3. N4 ratio evaluation

Superlatively, the FTIR spectra is usually deconvoluted to ascertained N4 ratio. De-convolution technique allowed assessing the comparative area (A) of each component which is directly proportional to the content of structural groups. Thus, this ratio is estimated by using the following expression [20]:

$$N_4 = \frac{A_4}{A_4 + A_3} \tag{8}$$

Herein, the relative peaks under BO_4 and TeO_4 is denoted by A_4 while A_3 are those that fall under TeO_3 and BO_3 units.

3. Results and discussion

3.1. XRD profile validation

Illustratively, the plot of XRD pattern for glass C is depicted in Fig. 1. Obviously, the XRD profile recorded from 10 to 80° zone does not exhibit any diffraction peaks but only humps around 2θ ~ 20-35° which certify the glassy state of the prepared glasses. Besides, numerous amorphous materials as studied and publicized by distinguished scholars divulged an exclusive scattering profile due to modifications in short range structural order [26], [27], [28].

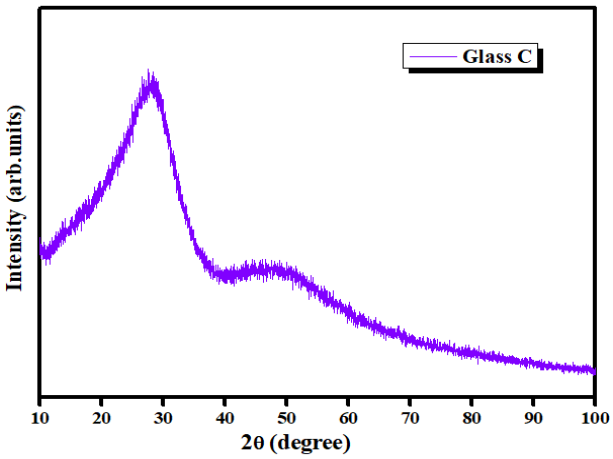

Fig. 1. XRD Profile of glass C sample.

3.2. Numerical analysis of physical properties

Herein, a number of physical quantities were computed for the whole glass samples and the achieved data are registered in Table 1. Profoundly, the glass density is documented as one of the key physical entity which other crucial physical parameters relied [29]. Fig. 2 publicized the trend of molar volume and density with increasing Sm_2O_3 content. Noticeably, a gradual substitution of B_2O_3 by Sm_2O_3 enhanced the density of the glasses with a notable reduction in the molar volume. The realistic augmentation in the density is attributed to the projected exchange among boron atoms and samarium ions owing to the discrepancy in their atomic numbers (samarium with 62≥5 for boron) [30]. Assertively, the empirical decline in the molar volume with rise in Sm_2O_3 content signposted the compactness of the studied glasses. Other computed values of physical parameters including sm^{3+} ions concentration, r_p, r_i, and F of the present glass compositions were compiled in Table 1 and their corresponding plots as functions of samarium concentration is well presented in Fig. 3 and 5, correspondingly. Apparently, both Sm^{3+} ions concentration and F depicted in Fig. 3 increased linearly with upturn in the Sm_2O_3 content, whereas the values of both $r_p$and r_i diminishes (see Fig. 4). This verdict is logical since the atomic radius of samarium (242 pm) is larger than that of the boron (85 pm) [31]. The decrement in the $r_p$and $r_i$and the improved values of F affirmed strong connection between Sm–O, which in turn produces stronger filed around Sm^{3+} ions.

Table 1. Acquired physical parameters of the present glass samples.

Glasses	Physical parameters					
	d_s (gcm^{-3})	V_m (cm^3mol^{-1})	Sm^{3+} $N_i \times 10^{21}$ions cm^{-2}	r_p(Å) $\times 10^{-8}$	r_i(Å) $\times 10^{-8}$	F $\times 10^{16}cm^{-2}$
Glass A	3.194	42.427	0.710	2.133	5.291	1.385
Glass B	3.387	40.180	1.049	1.873	4.646	1.796
Glass C	3.460	39.584	1.521	1.655	4.105	2.300
Glass D	3.536	38.980	2.008	1.509	3.743	2.767
Glass E	3.646	37.963	2.379	1.426	3.537	3.098

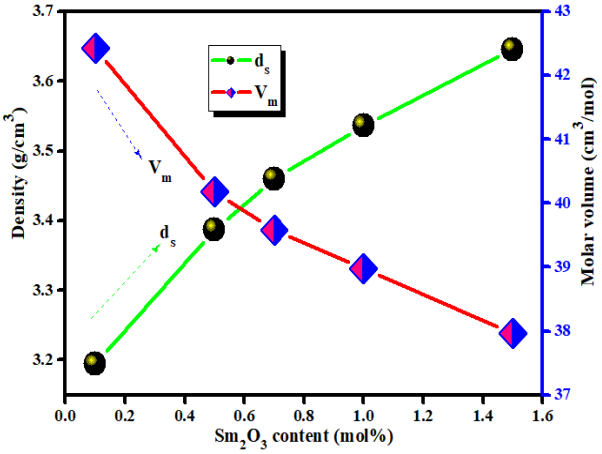

Fig. 2. The trend of density and molar volume with varying content of Sm_2O_3 in the present glasses: Lines are drawn as guides to the eyes.

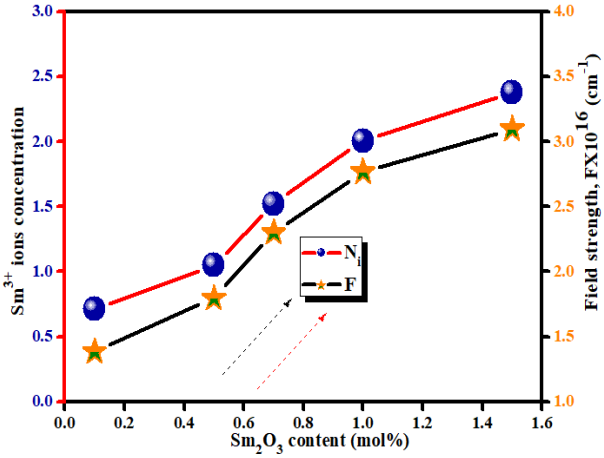

Fig. 3. A plot of Sm^{3+} ions concentration alongside field strength with increasing content of Sm_2O_3 in the present glass matrix: Lines are drawn as guides to the eyes.

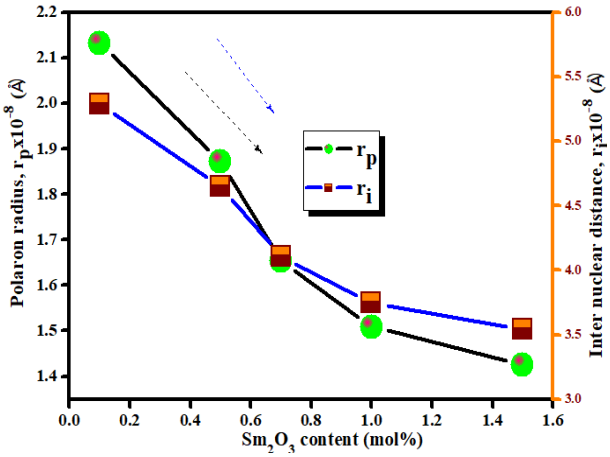

Fig. 4. A graph of polaron radius and inter-nuclear distance versus varying content of Sm_2O_3 in the present glass host: Lines are drawn as guides to the eyes.

3.3. Micro-hardness scrutiny of the present glasses

Contentedly, the inspection of micro-hardness provides some elementary facts on material resistance to permanent deformation made by harder material under stress [32]. In same base, the capability of any matter to withstand plastic or permanent deformation under concentrated mechanical loading is known as micro-hardness [32]. Further, hardness cannot be obviously defined as a physical property of a substance rather regarded as complex property of a material, which relies on the measuring conditions [19]. Thus, there are many routes for hardness inspection but herein, the classic Vickers hardness test approached was utilized with 50, 100, 200, 300 and 500 g applied weight and the acquired values of the hardness for studied glasses are compiled in Table 2. In general sense, the hardness of the glasses increases with decrease in NBO in the investigated glasses [33]. The experiential upsurge in H_V is accredited to the upsurge in rigidity of the network with formation of more BO in glasses. In this work, the attained hardness values with applied load is well exemplified in Fig. 4 and the experimental outcome are discussed by considering three zones as follows:

i. Lower applied load zone (zone I to zone II): This county is load dependent non-linear in nature and is primarily known as active zone.

ii. Upper applied load zone (zone II to zone III): This neighbourhood is load independent and is nearly constant in nature, principally, known as plateau or saturation zone.

Affirmatively, at lesser applied load region, the augmentation in hardness from I to II means that our fabricated glasses can withstand an applied force from 0.5 to 2.8 N. Afterwards, an extreme point of the plastic zone is expected to reach at around 3.0 N known as the plateau limit of hardness. This implied that further addition of applied load beyond this limit may lead to the glass samples softening [33].

Table 3. Load-dependent hardness of the present glass system.

Applied load (F)		**Hardness, H_V (GPa)**					
(g)	**(N)**						
Glasses			Glass A	Glass B	Glass C	Glass D	Glass E
50	0.490		0.608	0.896	1.224	2.311	3.110
100	0.980		0.851	1.107	1.761	2.807	3.624
200	1.960		1.295	1.563	2.139	3.095	4.063
300	2.940		1.718	1.995	2.160	3.300	4.370
500	4.900		1.940	2.163	2.198	3.462	4.409

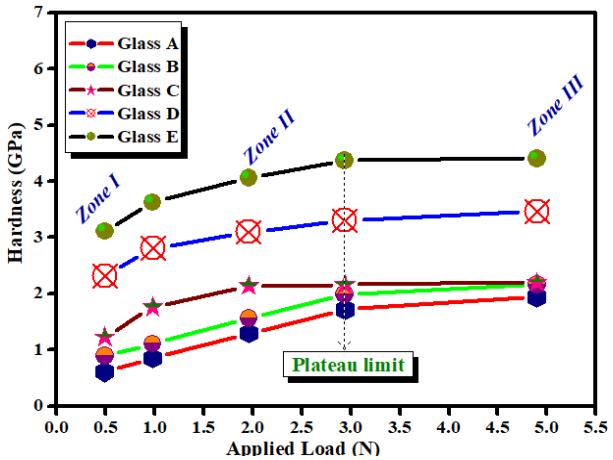

Fig. 5. A graph, disclosing hardness trend in the studied glasses as a function of applied load.

3.4. Inspection and identification of functional groups in the studied glasses

The research on Infrared absorption measurements is crucial for identifying the structural groups (BO_3, BO_4, PO_4, TeO_3, TeO_4, etc.) that are obtainable in the structure of the present zinc telluro-phospho-borate systems. Therefore, the FTIR spectra acquired within 400-1600 cm^{-1} spectral zone is depicted in Fig. 5.

3.4.1. Revelation of FTIR spectral peaks of the studied glasses

Herein, it is worth mentioned that our newly fabricated parent glass comprises of three unified glass forming oxides such as TeO_2, P_2O_5 and B_2O_3 possessing 30%, 10% and 50% component constituents, respectively. In this basis, the observed IR vibrational modes is anticipated to unveiled the structural network of borate, phosphate and tellurite network. To interpret the detected absorption spectral bands, it is important to take note of the following parameters:

i. A theory hosted by the famous researchers namely Tarte and Condrate [34] on the free independent vibrations of the entire constituent's units regardless the existence of other different groups. The similar model has been sequentially implemented by Rai et al. [35]

ii. The central structural vibrations are anticipated to be from borate network since it occupies 50% in the glass composition. Further, the structure of B_2O_3 is reformed with the introduction of samarium oxide (Sm_2O_3). In general, the addition of modifying oxide into B_2O_3 results in transformation from BO_3 to BO_4 units and vice versa [36].

In line with the existence literature, the following explanations are made for our experiential FTIR spectra.

a) The broad band centre around 530 cm^{-1} are ascribed to the vibrations of the Te–O bonds between TeO_4 and bending vibration of P_2O_5 [37]

b) The left shoulder band at ~953 cm^{-1} are allocated to widening modes of B–O bonds in BO_4 units from tri-, tetra- and penta-borate groups [38]

c) The practical peak around ~1075 cm^{-1} is interconnected to the symmetrical stretching vibration of PO_4 groups [39]

d) The noted peak at ~1200 cm^{-1} is an ultimate widening modes of B -O bonds in BO_4 units [40]

e) The realistic band centre ~1452 cm^{-1} is an indicative of the Stretching vibrations of B–O bonds in BO_3 units from metaand ortho -borate groups [39]

f) The notable band at 1642 cm^{-1} signals the existence of B-O-H bridge, OH bending vibration [41]

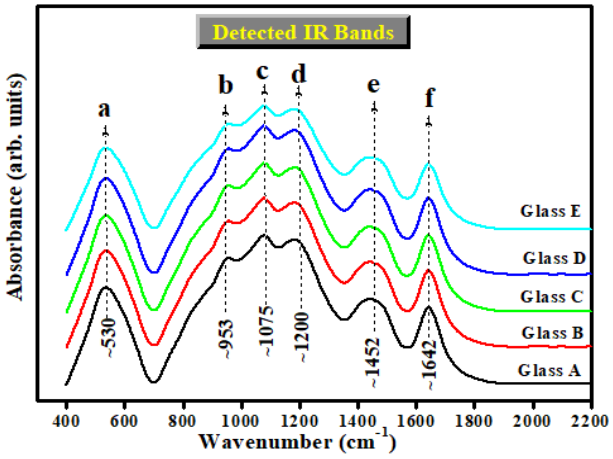

Fig. 6. FTIR spectra of the present glasses.

Table 3. The acquired FTIR spectra bands, positions and assignments of the present glasses.

Detected band	Detected band position (cm^{-1})					Bands Assignments
	Class A	Class B	Class C	Class D	Class E	
a	535	535	527	530	530	Te–O bonds between TeO_4 [42], [43]
b	943	947	947	943	953	stretching vibrations of B–O bonds in BO4 units [42]
c	1075	1075	1078	1071	1078	symmetrical stretching vibration of PO4 groups [44], [45]
d	1203	1192	1196	1185	1192	Twisting modes of B−O−B in [BO4] units [46]
e	1448	1459	1452	1445	1459	Widening vibrations of B−O of BO_3 units in metaborate, pyroborate and orthoborate groups [47], [16]
f	1639	1642	1642	1639	1642	B-O-H bridge, OH bending vibration [48]

3.3.2. N4 ratio scrutiny

A quantitative scrutiny of the FTIR spectra (Fig. 6) was conducted by mindfully deconvoluted the IR using PeakFit program route to unveils some hidden bands at wavenumbers different from local maximum in the data stream. Therefore, by employing a crucial expression described elsewhere in [49], [50] and also in Eqn. 8 of this work. The N_4 ratio was duly computed and the attained values are tabulated in Table 4. Further, the corresponding N4 ratio plot as function of Sm2O3 content is depicted in Fig. 8. Apparently, TeO_4 and BO_4 and PO4 units upturns with augmentation in Sm_2O_3 content. This decree indeed authenticate tightly packed structure due transformation of $BO_3 \rightarrow$ BO4, $TeO_3 \rightarrow$ TeO4 alongside the occurrence of PO_4.

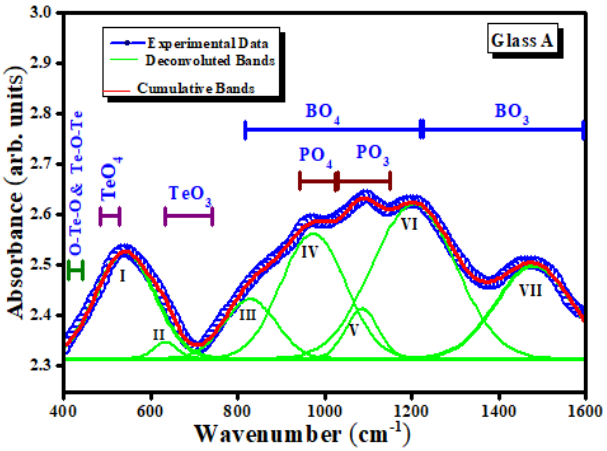

Fig. 7. A typical deconvolution of IR spectra of glass C sample deduced by using a Gaussian-type function.

Table 4. Attained comparative areas of deconvoluted IR bands together with N_4 ratio for BO_4, TeO_4 and PO_4 units in present glasses.

Sample	Comparative areas of the FTIR bands							BO_4 Ratio	TeO_4 Ratio	PO_4 Ratio
	I at ~513 cm^{-1}	**II** at ~630 cm^{-1}	**III** at ~800 cm^{-1}	**IV** at ~940 cm^{-1}	**V** at ~1070 cm^{-1}	**VI** at ~1190 cm^{-1}	**VII** at ~1450 cm^{-1}	$\frac{III+VI}{III+VI+VII}$	$\frac{I}{I+II}$	$\frac{IV}{IV+V}$
Glass A	30.011	5.179	11.190	33.073	9.001	71.836	39.405	0.678	0.853	0.786
Glass B	30.979	5.297	20.281	39.823	10.806	72.262	39.433	0.701	0.854	0.787
Glass C	30.590	5.135	26.575	39.292	9.110	73.527	41.309	0.708	0.856	0.812
Glass D	31.967	4.963	26.633	39.917	7.864	73.265	40.839	0.710	0.866	0.835
Glass E	31.787	4.522	17.831	37.343	6.697	57.321	29.174	0.720	0.875	0.848

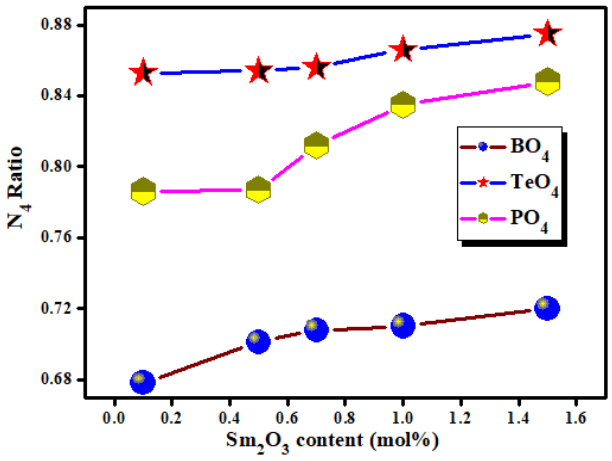

Fig. 8. Correlation between N_4 ratios (BO4, TeO4 and PO4) with increasing Sm2O3 content (mol%).

4. Conclusion

Convincingly, five samples of glasses (A, B, C, D and E) were used in this study to ascertain the role of Sm_2O_3 on the physical and mechano-structural properties of $(50\text{-}x)B_2O_3\text{-}10P_2O_5\text{-}30TeO_2\text{-}10ZnO\text{-}xSm_2O_3$ with x = 0.1, 0.5, 0.7, 1.0 and 1.5 mol%. On the physical attributes, the density of all studied samples disclosed a steady augmentation while the molar volume decreases due to substitution of light element (Boron) by heavy element (Samarium). Besides, micro-hardness analysis publicized closely packed structure in the present glasses. This disclosure was further certified by the FTIR and deconvoluted spectra scrutiny wherein BO_3, TeO_3 are transformed to BO_4, TeO_4 alongside the appearance of PO_4 with formation of more bridging oxygens. These advantageous properties exhibited by the present glasses are highly desirable in high strength glasses.

Acknowledgements

The authors appreciate Princess Nourah Bint Abdulrahman University Research Supporting Project Number (PNURSP2024R479), Princess Nourah Bint Abdulrahman University, Riyadh, Saudi Arabia.

References

[1] Farhan, S.H., Al Dabbagh, B.M., Aboud, H., Chalcogenide Letters, Vol, 21 no. 6, pp.459-473, 2024; https://doi.org/10.15251/CL.2024.216.459

[2] Bulus, Ibrahim, Areej S. Alqarni, N. N. Yusof, Muneerah Alomar, Materials Chemistry and Physics 309, pp 128322, 2023; https://doi.org/10.1016/j.matchemphys.2023.128322

[3] El Jouad, Mohamed, Samira Touhtouh, Otmane Sadek, Abdelowahed Hajjaji, Materials Today: Proceedings 66, pp 349-352, 2022; https://doi.org/10.1016/j.matpr.2022.05.450

[4] S. Hathot, B. Al Dabbagh, H. Aboud, Chalcogenide Letters, vol. 21, no. 2, 2024; https://doi.org/10.15251/CL.2024.212.201

[5] Abuallan, Mohammad Ayman, Mohd Hafiz Mohd Zaid, Khamirul Amin Matori, Yazid Yaakob, Abdul Rahman Sarmani, Wei Mun Cheong, Zhi Wei Loh, Materials Today Communications 36 pp 106599, 2023; https://doi.org/10.1016/j.mtcomm.2023.106599

[6] Zaitizila, I., M. K. Halimah, F. D. Muhammad, M. S. Nurisya. Journal of Non-Crystalline Solids 492, pp 50-55, 2018; https://doi.org/10.1016/j.jnoncrysol.2018.04.019

[7] Cardillo, E.C., M.A. Frechero, Optical Materials, 149: p. 114878, 2024; https://doi.org/10.1016/j.optmat.2024.114878

[8] Wan, Rui, Chen Guo, Xianda Li, Pengfei Wang, Ceramics International Vol. 50, no. 4, pp 7168-7176, 2024; https://doi.org/10.1016/j.ceramint.2023.12.085

[9] Abdullahi, I., S. Hashim, M. I. Sayyed, S. K. Ghoshal, Heliyon Vol. 9, no. 5, 2023; https://doi.org/10.1016/j.heliyon.2023.e15906

[10] Mošner, Petr, Kateřina Vosejpková, Ladislav Koudelka, Lionel Montagne, Bertrand Revel, Materials Chemistry and Physics 124, no. 1, pp 732-737, 2010; https://doi.org/10.1016/j.matchemphys.2010.07.048

[11] Mošner, P., K. Vosejpková, L. Koudelka, L. Beneš, Journal of Thermal Analysis & Calorimetry Vol. 107, no. 3, 2012; https://doi.org/10.1007/s10973-011-1535-4

[12] Selvi, S., Godugunuru Venkataiah, S. Arunkumar, G. Muralidharan, K. Marimuthu, Physica B: Condensed Matter 454, pp 72-81, 2014; https://doi.org/10.1016/j.physb.2014.07.018

[13] Selvi, Structural, K. Marimuthu, G. Muralidharan, Journal of Luminescence 159, pp 207-218, 2015.5; https://doi.org/10.1016/j.jlumin.2014.11.025

[14] Selvi, S., K. Marimuthu, N. Suriya Murthy, G. Muralidharan, Journal of Molecular Structure 1119, pp 276-285, 2016; https://doi.org/10.1016/j.molstruc.2016.04.073

[15] Qian, Zhicheng, Jun Cai, Changyuan Li, Zhihong Zhang, Jianhua Wang, Radiation Physics and Chemistry 185, pp 109516, 2021; https://doi.org/10.1016/j.radphyschem.2021.109516

[16] Poojha, MK Komal, K. A. Naseer, Hanan Al-Ghamdi, Aljawhara H. Almuqrin, M. I. Sayyed, K. Marimuthu, Optik 264, pp 169433, 2022; https://doi.org/10.1016/j.ijleo.2022.169433

[17] Prabhu, Nimitha S., Vinod Hegde, Akshatha Wagh, M. I. Sayyed, O. Agar, Sudha D. Kamath, Journal of Non-Crystalline Solids 515, pp 116-124, 2019; https://doi.org/10.1016/j.jnoncrysol.2019.04.015

[18] Rajagukguk, Juniastel, Nursaida Harahap, Rahmaniar, Rappel Situmorang, Abd Hakim S, Sunaryono, Integrated Ferroelectrics Vol. 214, no. 1, pp 143-150, 2021; https://doi.org/10.1080/10584587.2020.1857190

[19] Zalamin, S. N. F., MH M. Zaid, K. A. Matori, M. K. A. Karim, Y. Yaakob, W. M. Cheong, Z. W. Loh, M. I. Sayyed, Progress in Nuclear Energy 161, pp 104752, 2023. https://doi.org/10.1016/j.pnucene.2023.104752

[20] Bulus, Ibrahim, R. Hussin, S. K. Ghoshal, Abd R. Tamuri, S. A. Jupri, Ceramics International Vol. 45, no. 15, pp 18648-18658, 2019; https://doi.org/10.1016/j.ceramint.2019.06.089

[21] Teresa, P. Evangelin, R. Divina, K. A. Naseer, K. Marimuthu, Optik 259, pp 169024, 2022; https://doi.org/10.1016/j.ijleo.2022.169024

[22] Alsaif, Norah AM, Hanan Al-Ghamdi, R. A. Elsad, A. M. Abdelghany, Shaaban M. Shaaban, Y. S. Rammah, Islam M. Nabil, Journal of Materials Science: Materials in Electronics Vol. 35, no. 7, pp 534, 2024; https://doi.org/10.1007/s10854-024-12290-4

[23] Mhareb, M.H.A., Applied physics A, 126, pp 1-8, 2020; https://doi.org/10.1007/s00339-019-3262-9

[24] Eraiah, B., Journal of Non-Crystalline Solids, 551: pp 120394, 2021; https://doi.org/10.1016/j.jnoncrysol.2020.120394

[25] Madshal, M. A., G. El-Damrawi, A. M. Abdelghany, M. I. Abdelghany, Journal of Materials Science: Materials in Electronics Vol. 32, no. 11, pp 14642-14653, 2021; https://doi.org/10.1007/s10854-021-06022-1

[26] Bulus, I., J. K. Sheyin, E. Yayock, A. S. Dalhatu, Open Journal of Physical Science, Vol. 1, no. 1, pp 1-10, 2020; https://doi.org/10.52417/ojps.v1i1.84

[27] Albaqawi, Hissah Saedoon, S. M. Al-Shomar, Ibrahim Mohammed Danmallam, Ibrahim Bulus, Journal of Alloys and Compounds 965, pp 171101, 2023; https://doi.org/10.1016/j.jallcom.2023.171101

[28] Vedavyas, S., Islam M. Nabil, K. Chandra Sekhar, N. Almousa, Shams AM Issa, Md Shareefuddin, Hesham MH Zakaly, Optical Materials 150, pp 115157, 2024; https://doi.org/10.1016/j.optmat.2024.115157

[29] Wantana, N., E. Kaewnuam, Y. Ruangtaweep, P. Kidkhunthod, H. J. Kim, S. Kothan, J. Kaewkhao, Radiation Physics and Chemistry 172, pp 108868, 2020; https://doi.org/10.1016/j.radphyschem.2020.108868

[30] Kilic, Gokhan, Shams AM Issa, Erkan Ilik, O. Kilicoglu, H. O. Tekin, Ceramics International Vol. 47, no. 2, pp 2572-2583, 2021; https://doi.org/10.1016/j.ceramint.2020.09.103

[31] Al-Hadeethi, Yas, M. I. Sayyed, J. Kaewkhao, A. Askin, Bahaaudin M. Raffah, E. M. Mkawi, R. Rajaramakrishna, Applied Physics A 125, pp 1-7, 2019; https://doi.org/10.1007/s00339-019-3115-6

[32] Shinozaki, Kenji, Tsuyoshi Honma, Takayuki Komatsu, Materials Research Bulletin Vol. 46, no. 6, pp 922-928, 2011; https://doi.org/10.1016/j.materresbull.2011.02.031

[33] Bulus, Ibrahim, Areej S. Alqarni, Abd Rahman Tamuri, S. K. Ghoshal, Ibrahim Mohammed Danmallam, Abdullahi Anderson Kassimu, Journal of Taibah University for Science Vol. 17, no. 1, pp 2178165, 2023; https://doi.org/10.1080/16583655.2023.2178165

[34] Marzouk, M., F. ElBatal, H. ElBatal, Silicon, Vol. 10: pp 615-625, 2018; https://doi.org/10.1007/s12633-016-9503-z

[35] Rai, V.N., S.N. Thakur, Photoacoustic and Photothermal Spectroscopy.Elsevier pp 281-305, 2023; https://doi.org/10.1016/B978-0-323-91732-2.00028-8

[36.] Januchta, Kacper, Randall E. Youngman, Lars R. Jensen, Morten M. Smedskjaer, Journal of Non-Crystalline Solids 520, pp 119461, 2019; https://doi.org/10.1016/j.jnoncrysol.2019.119461

[37] Poojha, MK Komal, M. Vijayakumar, P. Matheswaran, K. Marimuthu, Optics & Laser Technology 156, pp 108585, 2022; https://doi.org/10.1016/j.optlastec.2022.108585

[38] Gowda, GV Jagadeesha, C. Devaraja, B. Eraiah, A. Dahshan, S. N. Nazrin, Journal of alloys and compounds 871, pp 159585, 2021; https://doi.org/10.1016/j.jallcom.2021.159585

[39] Priya, M., M. Dhavamurthy, A. Antony Suresh, M. Manoj Mohapatra, Optical Materials 142, pp 114007, 2023; https://doi.org/10.1016/j.optmat.2023.114007

[40] Queiroz, M. N., N. F. Dantas, D. R. N. Brito, M. J. Barboza, A. Steimacher, F. Pedrochi, Journal of Electronic Materials 48, pp 1643-1651, 2019; https://doi.org/10.1007/s11664-018-06893-x

[41] Lira, A., G. V. Vázquez, I. Camarillo, U. Caldiño, J. Orozco, J. L. Ruvalcaba, M. Manrique Ortega, Journal of Luminescence 255, pp 119545, 2023; https://doi.org/10.1016/j.jlumin.2022.119545

[42] D'Silva, A. Josuva, K. Maheshvaran, AJ Clement Lourduraj, I. Arul Rayappan, Journal of Materials Science: Materials in Electronics Vol. 34, no. 3 pp 212, 2023; https://doi.org/10.1007/s10854-022-09601-y

[43] Rao, Puli Nageshwer, K. Chandra Sekhar, T. Ramesh, M. Chandra Shekhar Reddy, Kodumuri Veerabhadra Rao, Md Shareefuddin, B. Appa Rao, Journal of Materials Science: Materials in Electronics Vol. 34, no. 25, pp 1756, 2023; https://doi.org/10.1007/s10854-023-11165-4

[44] Indhrapriyadarshini, A., K. A. Naseer, MK Komal Poojha, K. Marimuthu, M. I. Sayyed, Mohammed S. Alqahtani, Optik pp 171755, 2024; https://doi.org/10.1016/j.ijleo.2024.171755

[45] Al-Ghamdi, Hanan, Norah AM Alsaif, F. Afaneh, Z. Y. Khattari, A. M. Abdelghany, Y. S. Rammah, Optical and Quantum Electronics Vol. 55, no. 11, pp 1025, 2023; https://doi.org/10.1007/s11082-023-05362-y

[46] Karthika, S., S. Shanmuga Sundari, K. Marimuthu, P. Meena, Chemical Physics Impact Vol. 8, pp, 100430, 2024; https://doi.org/10.1016/j.chphi.2023.100430

[47] Al-Ghamdi, Hanan, Norah AM Alsaif, Z. Y. Khattari, R. A. Elsad, Adel M. El-Refaey, M. S. Sadeq, Y. S. Rammah, M. A. El-Shorbagy, M. S. Shams, Journal of Materials Science: Materials in Electronics Vol. 34, no. 14, pp 1180, 2023; https://doi.org/10.1007/s10854-023-10560-1

[48] Sasirekha, C., MK Komal Poojha, K. Marimuthu, M. Vijayakumar, Optical Materials 141, pp 113917, 2023; https://doi.org/10.1016/j.optmat.2023.113917

[49] Sadeq, M., M. Abdo, Ceramics International, Vol. 47, no. 2, pp 2043-2049, 2021; https://doi.org/10.1016/j.ceramint.2020.09.036

[50] Sadeq, M., M. AlHammad, R. Al-Wafi, Ceramics International, Vol. 50, no. 1, pp 115-125, 2024; https://doi.org/10.1016/j.ceramint.2023.10.028